High frequency surface acoustic wave resonator-based sensor for particulate matter detection

Thomas, S., Cole, M., Villa-López, F. H. & Gardner, J. W.

DOI 10.1016/j.sna.2016.04.003
ISSN 0924-4247
Publisher: Springer

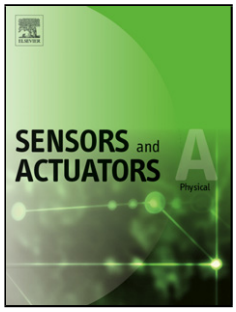

Title: High Frequency Surface Acoustic Wave Resonator-based Sensor for Particulate Matter Detection

Author: Sanju Thomas Marina Cole Farah H. Villa-López Julian W. Gardner

PII: S0924-4247(16)30148-0
DOI: http://dx.doi.org/doi:10.1016/j.sna.2016.04.003
Reference: SNA 9587

To appear in: *Sensors and Actuators A*

Received date: 23-6-2015
Revised date: 22-1-2016
Accepted date: 4-4-2016

Please cite this article as: Sanju Thomas, Marina Cole, Farah H.Villa-López, Julian W.Gardner, High Frequency Surface Acoustic Wave Resonator-based Sensor for Particulate Matter Detection, Sensors and Actuators: A Physical http://dx.doi.org/10.1016/j.sna.2016.04.003

High Frequency Surface Acoustic Wave Resonator-based Sensor for Particulate Matter Detection

Sanju Thomas, Marina Cole, Farah H. Villa-López and Julian W. Gardner

Microsensors and Bioelectronics Laboratory, School of Engineering, University of Warwick, Coventry, UK, CV4 7AL

S.Thomas.1@warwick.ac.uk, Marina.Cole@warwick.ac.uk, F.H.Villa-Lopez@warwick.ac.uk, J.W.Gardner@warwick.ac.uk.

Corresponding author: Julian W. Gardner,
School of Engineering, University of Warwick, Coventry, UK, CV4 7AL
J.W.Gardner@warwick.ac.uk

+ ŁÆª °ŁÆª –¹#

- New SAWR based particle sensor, capable of detection of sub-micron size particles with masses below 1 *ng*.
- Sensitive, low-cost and robust acoustic sensor for particulate matter (PM10, PM2.5, UFP) detection for air-quality monitoring.
- Novel SAWR design with free and shorted sensing areas, used in differential mode of operation.
- Potential for low-power monolithic CMOS implementation.
- Frequency dependent sensitivity of SAW resonators can be tailored to the size of particles to make them capable for UFPs, $PM_{2.5}$ and PM_{10} detection.

Abstract: This paper describes the characterization of high frequency Surface Acoustic Wave Resonator-based (SAWR) sensors, for the detection of micron and sub-micron sized particles. The sensor comprises two 262 MHz ST-cut quartz based Rayleigh wave SAWRs where one is used for particle detection and the other as a reference. Electro-acoustic detection of different sized particles shows a strong relationship between mass sensitivity $(\Delta f/\Delta m)$ and particle diameter (D_p). This enables frequency-dependent SAWR sensitivity to be tailored to the size of particles, thus making these types of sensors good candidates for PM_{10}, $PM_{2.5}$ and ultrafine particle (UFP) detection. Our initial characterisation demonstrated a typical SAWR frequency shift of 60 Hz in response to a deposition of *ca*. 0.21ng of 0.75 µm-sized gold particles (~50 particles) on sensor's surface. Sensor responses to different size particles, such as ~30 µm diameter silicon, gold (diameters of ~0.75 µm and ~20 µm), ~8 µm fine sugar, PTFE (~1 µm and ~15 µm), ~4 µm talcum powder, and ~2 µm molybdenum powder were evaluated, and an average mass sensitivity of 275 Hz/ng was obtained. Based on the results obtained in this study we believe that acoustic wave technology has great potential for application in airborne particle detection. Moreover, acoustic resonator devices can be integrated with CMOS interface circuitry to obtain sensitive, robust, low-power and low-cost particle detectors for variety of applications including outdoor environmental monitoring.

Keywords: Particulate matter detection; surface acoustic wave resonator; particle sensor; ultrafine particles; high frequency SAWR Sensor; PM_{10}; $PM_{2.5}$

1 Introduction

Air pollution is a common problem in both developed and developing countries and it has a major effect on human health. Particulate matter, carbon monoxide, ozone, nitrogen dioxide and sulphur dioxide are some of the major pollutants affecting human health. Small airborne particulate matter having diameters of 10 µm or less are commonly classified as PM_{10} (defined as particles equal to and less than 10 µm in diameter), $PM_{2.5}$ (defined as fine particles that consist of particles equal to or less than 2.5 µm in diameter) and UFPs (defined as particles with an aerodynamic diameter smaller than 0.1 µm). The latter ones are of particular concern due to their ability to penetrate deep into the lungs and blood streams, causing major health related problems including DNA mutations, heart attacks, and premature deaths [1]. In addition, PM pollution also has various environmental effects including visibility impairment, acid rain causing damages to the natural ecosystem and aesthetic damage to buildings and monuments. Since, even at relatively low concentrations, the burden of air pollution on health and ecosystem is significant, effective management of air quality is absolutely necessary [2]. More stringent regulations for indoor and outdoor air quality have been introduced by various environmental agencies and research organisations worldwide in order to set air quality standards at the level that effectively protects both public health and welfare. The European Commission has adopted a Clean Air Policy Package in December 2013, consisting of a new Clean Air Programme for Europe with new air quality objectives for the period up to 2030. In this $PM_{2.5}$ exposure reduction target is set to reach 18 µg/m3 based on the average exposure indicator (AEI) [3]. As a result, there is an urgent need to identify and measure atmospheric PM (e.g. dust, soot, and pollen) by developing and

validating strategies and monitoring systems for air quality measurements based on the latest measuring techniques with low detection limits.

Currently, PM measurements are typically carried out using aerosol monitoring instruments based on the principles of optical absorbance and filtration, quartz crystal microbalance, light scattering and pulse counting, tapered element oscillating microbalance and gravimetry [4–8]. Despite the fact that the conventional PM sampling methods provide certain advantages including real time data with short time resolution (<1 h) [9], most of these prevailing systems are bulky, expensive, and energy inefficient. Recent advances in nanoparticle based technologies have generated an increased interest in the development of smart, compact and low cost sensors for the precise measurement of ultra-fine particles including PM_{10} and $PM_{2.5}$.

This paper outlines development of a two-port SAWR-based particle microsensor. High frequency SAWRs are well known to be simple devices that are very sensitive to mass loading, with mass sensitivity levels several times higher than that of a quartz crystal microbalance (QCM) devices [10], [11]. In addition, they can be operated with low cost drive and signal conditioning circuitry, unlike optical devices which require sophisticated and expensive setups. The particle sensor described here is Rayleigh wave surface acoustic wave device capable of detecting micron and submicron sized particles, using sensitivity-tailored frequency-dependant designs of acoustoelectric sensors. The main advantages of SAWR devices include a simple and low cost fabrication procedure, high sensitivity and a fast response time, in addition to their compact size and robustness [12].

2 SAWR Sensor Theory and Principle of Operation

In this paper, we present the characterization of a novel, miniaturised particle detection sensor using a conventional high frequency two-port surface acoustic wave resonator operating in an oscillator configuration. The basic configuration of a SAWR sensor shown with sub-micron sized particles deposited on the active sensing area is illustrated in Figure 1. The figure depicts a device based upon a piezoelectric substrate with inter-digital-transducers (IDT) and reflectors on each side of the device patterned in order to produce a standing Rayleigh-type acoustic wave.

(Figure 1 near here)

For a Rayleigh SAWR sensor, the sensing region lying between the two IDTs constitutes the central mass sensitive region referred to here as the active area. The reflector gratings on both sides of the SAWR IDTs form a resonant acoustic cavity. At the resonant frequency, this cavity will trap the acoustic wave in the form of standing waves between the two reflector gratings. With diminished standing wave amplitude away from the SAWR central cavity gap (active area), remote reflector gratings have a smaller effect on the resonator frequency [13]. Thus, the sensitivity will be highest at the central active area between the two IDTs.

When the particles fall on the sensor surface the propagation of the acoustic waves is perturbed and as a result, both the velocity and attenuation of the wave change. If the devices

are placed in an oscillator configuration these changes can be measured with great accuracy as a change in resonant frequency. The sensing mechanism of the surface wave sensor depends on various factors including mechanical and electrical properties of the particles under test [14,15]. The mechanical effects include mass density and visco-elasticity of the particles, while the electrical effects include their conductivity and dielectric permittivity [16].

The theory behind SAWR sensors in general shows that SAW perturbations on a non-metallized active area, so-called *free* sensing area, are related to both the mechanical and the acoustoelectric properties of the adjacent medium [17]. However, by covering the sensing area with a thin conducting layer such as gold, an electrically-*shorted* SAWR device is formed, resulting in negligible effect due to electric potential [18]; therefore, the sensor response is dominated by only the mechanical properties of the medium under test. Thus for a *free* SAWR particle sensor, change in SAW frequency could be associated with the following variables including mass density ρ, viscosity η, conductivity σ, and dielectric permittivity ε of the particles under test. The total frequency shift, Δf, can be expressed using the differential theorem as shown below:

$$\Delta f_{Free} = \left\{ \frac{\partial f_{particle}}{\partial \rho_{particle}} \Delta \rho_{particle} + \frac{\partial f_{particle}}{\partial \eta_{particle}} \Delta \eta_{particle} + \frac{\partial f_{particle}}{\partial \sigma_{particle}} \Delta \sigma_{particle} + \frac{\partial f_{particle}}{\partial \varepsilon_{particle}} \Delta \varepsilon_{particle} \right\} \quad (1)$$

For an electrically *shorted* SAWR device, the electrical terms may be neglected thus leaving:

$$\Delta f_{Shorted} = \left\{ \frac{\partial f_{particle}}{\partial \rho_{particle}} \Delta \rho_{particle} + \frac{\partial f_{particle}}{\partial \eta_{particle}} \Delta \eta_{particle} \right\} \quad (2)$$

The difference between the two frequency parameters gives the electrical terms, thus permitting the separation out of both purely mechanical and purely electrical properties of the particles under test. In this work both configurations of the two-port SAWR devices were utilized: *free* (with non-metallized active areas) and *shorted* (with metallized active areas).

Depending on the nature of the SAWR sensor surface i.e. metallized (*shorted*) or non-metallized (*free*), the generated acoustic waves possess both mechanical and electrical penetration depths. That means that, when a Rayleigh wave is generated on a piezoelectric substrate, it has an associated acousto-electric potential that extends into the adjacent medium. It is the distance of this wave penetration (called skin or penetration depth), which determines how far into the adjacent medium a measurable property can be detected. In the case of particle sensors, the acousto-electric potential of the SAW sensor extends into the particulate matter and the extent of penetration of this potential determines how far from the sensor/particle interface electrical and mechanical properties of the deposited particles can be detected by the sensor.

For the case of a metallized device, the electrical penetration depth is negligible; as the device is electrically *shorted*. But for a *free* device, both the mechanical and electrical skin depths are visible. The electrical skin depth δ_e was calculated by Kondoh *et al.* [17] to be approximately $1/7^{th}$ of the SAWR sensor wavelength and is given by:

$$\delta_e = \lambda_0 / 7 \tag{3}$$

The effective mechanical penetration depth δ_m of a SAWR sensor is given by the equation [19]:

$$\delta_m = \sqrt{\frac{\eta}{\pi f_0 \rho}} \tag{4}$$

where η and ρ are the viscosity and density of the adjacent medium respectively, and f_0 is the resonant frequency of the device.

From the above two equations, it is obvious that the penetration depths are inversely proportional to the resonant frequency of the SAWR device and hence, the limit of particle detection using SAWR devices can be tailored to the particle diameters of interest by varying the resonant frequency of the sensor; thus in turn changing the penetration depths. In order to have an effective detection of UFPs, PM2.5 and PM10s, sensors with different operating frequencies need to be used having the optimal penetration depths to suite the size of the particles. Figure 2 shows the pictorial representation of a SAWR based sensor illustrating the mass detection mechanism for detection of particulate matter; shown with penetration depths extending into the adjacent medium.

(Figure 2 near here)

The change in resonant frequency of a SAWR due to mass loading (neglecting the viscoelastic and electrical effects) has been characterized by the classic Sauerbrey equation, which is given by

$$\Delta f = -\frac{2 f_0^2}{\sqrt{\rho_s \mu_s}} \frac{\Delta m}{A} \tag{5}$$

where f_0 is the resonant frequency of the SAW device, A is the active area of the sensor, ρ_s is the substrate density, ρ_s is the substrate shear modulus and Δm is the change in mass.

The above formula will be used to calculate mass sensitivities of *free* and *shorted* SAWR devices due to mass loading of different types of particles.

3 Materials and Methods

3.1 SAWR Particle Sensor Design

The particle sensors were designed to resonate at a frequency of 262 MHz (optimised for the acoustic penetration depth of ~3 μm). They were made up of aluminium based inter-digital-

transducers (IDTs) patterned on top of ST-cut quartz substrate, resulting in generation of Rayleigh waves propagating in the crystallographic X-direction. The SAWR devices were fabricated at SAWTech (Germany) employing 4" ST-cut quartz wafers, using UV lithography. The IDTs consist of 60.5 finger pairs with 3 μm finger width. The acoustic aperture is 720 μm, while the cavity length is 1764 μm constituting an overall die size of 9.6 × 3.6 mm^2. The IDTs are surrounded by a total of 1200 reflector gratings (600 on each side) with 6 μm pitch, to create a standing wave pattern between the IDTs. ST-cut quartz substrates were chosen in order to eliminate the need for temperature control circuitry due to their high temperature stability.

The use of a reference sensor is a standard method of compensation, hence the SAWRs are employed to operate in a dual sensor configuration, as shown in Figure 3 [11,20]; where this differential structure provides better signal stability and reduced noise by compensating for atmospheric effects such as change in pressure, temperature, humidity and other common mode variations.

(Figure 3 near here)

The SAW sensors have been designed to resonate in a feedback loop of a simple radio frequency oscillator circuit at 262 MHz. Figure 4[A] shows a block diagram representation of the dual sensor and its associated interface circuitry.The characteristics of the SAW resonators are dependent upon the accuracy of the fabrication process; consequently, there can be variation between the designed electrical characteristics of frequency, attenuation, phase shift, input impedance and the actual obtained values. The S21 scattering parameter analysis shows that a maximum signal transmission occurs at 261.9 MHz frequency (as presented in Figure 4[B]) and shows good agreement with the SAWR design parameters. The acoustic wave attenuation at the IDT/substrate interface is very low [11] and the loss is only about 11 dB for the fabricated Rayleigh SAWR devices. As the SAW resonators were designed for both input and output impedances of 50 Ω, the need of additional impedance matching circuits were avoided.

(Figure 4 near here)

3.2 Oscillator Circuit

The choice of an optimal circuit to drive the SAWRs depends on the electrical characteristics of the fabricated resonator devices. In addition to the commonly used attenuation and phase based measurement techniques, SAWRs can be used for frequency based measurements when employed as frequency control elements in an oscillator circuit as shown in Figure 4. Detection of the micron and sub-micron sized particles is characterised by changes in the oscillator frequency of the SAWR oscillator system. A modular feedback based oscillator topology was chosen as this allows the 262 MHz SAWR to operate in a two-port configuration and also offers good stability and robustness at higher frequencies [21].

The oscillator was designed for operation in the 60 to 800 MHz frequency range, providing a wide-band, high gain capability. Low power RF Amplifiers (μPC2710, NEC) which are matched to 50 Ω internally provide required gain to compensate for loop losses including

SAWR insertion loss, mass loading and filter losses. Passive low pass filter boards are used for noise reduction, phase tuning and overtone suppression at higher frequencies. An oscillator board containing the basic oscillator circuit components (i.e. inductors and capacitors) and boards containing the filter and the dual sensor has been implemented using a four layered PCB with separate grounding planes which reduces the radio frequency (RF) cross talk, thereby improving noise sensitivity [22]. A differential analogue output is provided by the buffer amplifier (μPC2711, NEC), which is sent to the commercial frequency counter interface board (JLM Innovation, Germany) that in turn connects to a computer USB port to perform data acquisition and processing. The dual two-port SAWR sensor (with reference channel) and the schematic of the associated electronic circuitry for excitation, amplification, buffering and read-out are shown in Figure 5[A], while the photograph of the entire sensor setup with surface mount amplifier, filter and buffer circuitry is shown in Figure 5[B].

(Figure 5 near here)

4 Experimental Procedure

The experimental setup for determining the particle detection capability of the SAWR sensor is shown in the Figure 6[A]. This setup consists of a precision linear translation stage (LS Starrett Co., USA), the SAWR particle sensor with the oscillator circuitry and a digital microscope (Dino-Lite Europe, The Netherlands), in addition to the commercial interface board for PC interfacing. The linear translational stage integrates three micrometres with 12.5 mm travel range along x, y and z axes and is connected to one end of a suspended metallic rod. The other end of this rod is attached to a 25 μm thick gold bondwire. The micro scale movement of the linear stage helps to move the bondwire in all the three axes for the accurate deposition of particles on to the sensor surface.

The bondwire is plunged into a bottle containing micrometre-sized particle powder (with known particle diameter) so that some particles adhere on to it due to the attractive interparticle forces that exist in micron and sub-micron sized particles [23]. With the aid of the linear translation stage, this bondwire (containing the adherent particles) is then gently rubbed onto the sensor surface, allowing the particles to fall on to the sensor surface. The deposition of this particle mass onto the sensor surface produces a shift in frequency at the SAWR oscillator output. The entire deposition process was visually monitored in real time through a digital microscope, to guide the placement of particulate mass on to the sensor surface. In addition, a photomicrograph of the sensor surface with the deposited particles was also captured, which was used to count the number of particles deposited onto the sensing area. Figure 6[B] shows the photograph of gold particles with diameter of < 1 μm deposited on the sensing area of the SAWR particle sensor. The scanning electron microscopic images of these gold particles are shown in Figure 6[C]. The sensor unit is placed inside an environmental chamber to ensure ambient temperature stability, to avoid both air current effects and the deposition of any foreign material on the sensor within the laboratory environment.

(Figure 6 near here)

5 Results and Discussion

In order to evaluate the particle sensing capability of the SAWR sensor and to establish the mass sensitivity of the sensor, different types of micro particles with known diameters were deposited on the different regions within the total sensor surface area (including the sensor active area, IDT regions, and reflector regions of the SAWR sensor). The different types of controlled artificial aerosols, with an aerodynamic diameter range of approximately 1 - 30 μm, were used in the characterisation of devices.

The metrics under investigation also included particle number and particle mass, in addition to the frequency shift observed from the SAWR sensor. The frequency response of the sensor is related to the number of particulate matter present on the sensor surface, which in turn depends on the particle diameter. The photograph of the sensor surface (with the deposited particles) was processed using the image processing and analysis software *ImageJ 1.46r* (National Institutes of Health, USA) in order to define the number of deposited particles; thereby determining the total mass deposited on the sensor surface. A typical free SAWR sensor response to the deposition of *ca*. 0.21ng of 0.75 μm-sized gold particles (~50 particles) on to the central active region of the sensor is shown in Figure 7[A], which produces a differential frequency shift of 60 Hz.

The artificial aerosols used in the investigation included silicon powder, fine sugar crystals, PTFE with two different diameter range, fine talcum powder, molybdenum micro particles and gold micro particles with 2 different diameters. As explained in SAWR theory Section 2, the total frequency shift of a SAWR device is dependent on different physical factors including mass density, viscosity, conductivity, and dielectric permittivity of the deposited particles (Eq.1 and 2); as a result, the frequency shift can be related to one or all of these dependent variables, depending on whether the active sensing area is *free* or *shorted*. Particles like PTFE (~1 μm diameter), molybdenum (~1.5 μm diameter) and talcum powder (~4 μm diameter) were deposited on to both *free* and *shorted* dual SAWR devices separately and the differential frequency shifts were recorded each time. The mass sensitivities have been calculated each time based on Eq. 5 and the Figure 7[B] shows the mass sensitivities obtained using these *free* and *shorted* SAWR devices for the above-mentioned particles. This figure shows that the frequency shift obtained for a *free* SAWR device is larger, when compared to a *shorted* device. This is because both the mechanical and electrical interactions contribute to the *free* SAWR measurement; while only mechanical effects contribute to the *shorted* SAWR response.

(Figure 7 near here)

In order to evaluate the particle sensing capability of the different sensor regions, the same type of particle mass (~0.75 μm diameter gold) have been deposited onto different locations (sensor active area, IDT regions, and reflector regions) on separate *free* SAWR devices; and the resulting mass sensitivity of the SAWR sensor was measured. The experimental data obtained show that mass sensitivity diminishes as expected, while moving away from the central sensing area towards the furthest reflector gratings. This sensitivity distribution follows the sensor position pattern as shown in the figure 8. From the figure, it is clear that the mass sensitivity will be at the maximum when the particles are deposited onto the central

cavity area (origin of x-axis) of the SAWR device, and it will be the minimum when the particles fall onto the far outer end of the reflectors.

(Figure 8 near here)

In order to establish the minimum sensitivity and the linearity of the sensors, the frequency response of the SAWR sensor was measured to various levels of particle concentration. In random trials, 0.75 μm sized gold particles were deposited on to the active area of a free 262 MHz SAWR device. As seen from Figure 9, the average SAW mass sensitivity to 0.75 μm sized gold particles is 250 - 275 Hz/ng and the response of the sensors is almost linear indicating the reliability of the sensor setup and confirming that the sensors operated in the non-saturated regime.

(Figure 9 near here)

For a Rayleigh wave surface acoustic wave devices, acoustic wave travel along the quartz substrate surface in a vertical plane. According to Gronewold [24], surface interactions occur in the close proximity of the SAWR sensor where there is an increased mass sensitivity behaviour. Hence during particle sensing, if the particle diameter is within the penetration depth of the SAWR device, then the entire particle will be probed, resulting in improved sensitivity. However, if the particle size is greater than the penetration depth of the device, then acoustic waves will not penetrate the region outside the penetration depth boundary; resulting in partial sensing of the particles.

Hence, in order to allow acoustic coupling of the entire particle volume, the particle size must be less than the acoustic penetration depth (~3 μm) of the designed SAWRs. Else, the sensor probes only a part of the particle near its surface. Thus, the SAWR sensitivity $\Delta f/\Delta m$ will be higher (in the range of Hz/ng) for particles having sizes smaller than the penetration depth, whilst the sensitivity will be much smaller (in the range of Hz/μg) for those particles with size range greater than the penetration depth. In order to confirm such device sensitivity/particle size dependency, initial experiments were conducted where the same types of particles with different diameters (one with size < penetration depth and another with size > penetration depth) were in turn deposited onto different *free* SAWR devices and the mass sensitivity was measured in each case. Figure 10[A] shows the sensitivity (log scale) obtained using two different types of particles (gold and PTFE) having diameters within and outside the penetration depth of the SAWR sensor.

Due to the strong dependency of particle number concentrations on the cut-off characteristic of the acoustic sensor, it is possible to optimize the sensor design for high frequency operation in order to achieve required sensitivity for particles with different aerodynamic diameter.

Mass sensitivities were obtained by depositing different types of particle masses with varying sizes like ~30 μm diameter silicon, gold (sizes of ~0.75 μm and ~20 μm), ~8 μm fine sugar, PTFE (~1 μm and ~15 μm), ~4 μm talcum powder, and ~2 μm molybdenum powder on to different SAWR devices. The relation between SAWR sensitivity $\Delta f/\Delta m$ and different

sized particles of one type has been established to be approximately a power law distribution on a log-log plot, where the sensitivity varies as a power of the particle diameter as shown in Figure 10[B]. The figure also shows the closeness of the experimental data to the power law fitting cure, which is a straight line.

(Figure 10 near here)

It could be observed that sensors exhibited higher mass sensitivity to particles of sizes smaller than penetration depth (~3 μm) thus confirming that sensors designed to operate at 262 MHz are optimised for $PM_{2.5}$ detection. This in turn confirms that the frequency-dependent sensitivity of the SAW resonators can be tailored to different particle sizes and therefore making them potentially capable of PM_{10} $PM_{2.5}$ and UFPs detection.

In order to further explore use of acoustic wave technology for particle detection experiments have also been carried out using Solidly Mounted Resonator (SMR) based bulk acoustic wave devices operating at much higher frequencies of 970 MHz. The results were benchmarked against two other commercial particle detectors (one optical and one QCM), using controlled aerosols and results are reported elsewhere [25] [26].

6 Conclusions and further work

We have presented development of a low cost and robust microsensor for particle detection based upon high frequency SAWR devices. A 262 MHz SAW particle sensor was found to be capable of detecting masses below 1 ng with a high mass sensitivity of 275 Hz/ng. The characterization of these SAWR based devices has been performed in laboratory conditions, in order to explore their sensitivity to particulate matter of different sizes and different composition (e.g. metal, insulator, organic etc.). This has furthermore helped to establish the relation between the mass sensitivity and particle size for the effective detection of micron and sub-micron particles. We have established that tailoring of the frequency-dependent sensitivity is possible, which makes SAW resonators promising technology for detection of PM_{10} $PM_{2.5}$ and UFPs.

Further work is being carried out on the development of a monolithic acoustic wave based particle sensors integrated with CMOS circuitry and designed for 3D-SiP solution whose sensitivity is determined by the operating frequency. The sensor design is being optimized for high frequency applications (~1 GHz) in order to achieve required sensitivity for possible application as a smart, low-cost PM monitor.

References

[1] United States Environmental Protection Agency, Particulate Matter, (2011). http://www.epa.gov/airquality/particlepollution/health.html (accessed June 17, 2015).

[2] World Health Organisation, Health effects of Particulate Matter, 2013. http://www.euro.who.int/__data/assets/pdf_file/0006/189051/Health-effects-of-particulate-matter-final-Eng.pdf.

[3] European Commission, Air Quality Standards, http://ec.europa.eu/environment/air/quality/standards.htm (accessed June 9, 2015).

[4] J.P. Black, MEMS-based system for particle exposure assessment using Thin-Film

Bulk Acoustic Wave Resonators and IR / UV optical discrimination, Ph.D Thesis, University of California at Berkeley, 2006.

[5] S. Steinle, S. Reis, C.E. Sabel, S. Semple, M.M. Twigg, C.F. Braban, et al., Personal exposure monitoring of PM2.5 in indoor and outdoor microenvironments, Sci. Total Environ. 508 (2015) 383–394. doi:10.1016/j.scitotenv.2014.12.003.

[6] D.C. Green, G.W. Fuller, T. Baker, Development and validation of the volatile correction model for PM10 - An empirical method for adjusting TEOM measurements for their loss of volatile particulate matter, Atmos. Environ. 43 (2009) 2132–2141. doi:10.1016/j.atmosenv.2009.01.024.

[7] H.S. Wasisto, S. Merzsch, A. Stranz, A. Waag, I. Kirsch, E. Uhde, et al., A resonant cantilever sensor for monitoring airborne nanoparticles, in: Transducers, Beijing, 2011: pp. 1116–1119. doi:10.1109/TRANSDUCERS.2011.5969233.

[8] A. Hajjam, J.C. Wilson, A. Rahafrooz, S. Pourkamali, Fabrication and characterization of thermally actuated micromechanical resonators for airborne particle mass sensing: II. Device fabrication and characterization, J. Micromechanics Microengineering. 20 (2010). doi:10.1088/0960-1317/20/12/125019.

[9] Air Quality Expert Group, Particulate Matter in the United Kingdom, Defra, London, 2005.

[10] W.D. Bowers, R.L. Chuan, T.M. Duong, A 200 MHz surface acoustic wave resonator mass microbalance, Rev. Sci. Instrum. 62 (1991) 1624–1629. doi:10.1063/1.1142442.

[11] S. Thomas, Z. Rácz, M. Cole, J.W. Gardner, Dual High-Frequency Surface Acoustic Wave Resonator for Ultrafine Particle Sensing, in: IEEE Sensors- Proc., Baltimore. MD, 2013: pp. 1–4. doi:10.1109/ICSENS.2013.6688319.

[12] J. Yang, Z. Rácz, J.W. Gardner, M. Cole, H. Chen, Ratiometric info-chemical communication system based on polymer-coated surface acoustic wave microsensors, Sensors Actuators B Chem. 173 (2012) 547–554. doi:10.1016/j.snb.2012.07.043.

[13] C.K. Campbell, Surface Acoustic Wave Devices for Mobile and Wireless Communications, Academic Press, San Diego., 1998. doi:10.1016/j.jacr.2012.01.004.

[14] C. Tasaltin, M.A. Ebeoglu, Z.Z. Ozturk, Acoustoelectric effect on the responses of saw sensors coated with electrospun ZnO nanostructured thin film, Sensors. 12 (2012) 12006–12015. doi:10.3390/s120912006.

[15] Z. Rácz, M. Cole, J.W. Gardner, M.F. Chowdhury, W.P. Bula, J.G.E. Gardeniers, et al., Design and umplementation of a modular biomimetic infochemical communication system, Int. J. Circuit Theory Appl. 41 (2013) 653–667. doi:10.1002/cta.1829.

[16] L. Fan, H. Ge, S. Zhang, H. Zhang, J. Zhu, Optimization of sensitivity induced by surface conductivity and sorbed mass in surface acoustic wave gas sensors, Sensors Actuators B Chem. 161 (2012) 114–123. doi:10.1016/j.snb.2011.09.077.

[17] J. Kondoh, Y. Matsui, S. Shiokawa, New biosensor using shear horizontal surface acoustic wave device, Jpn. J. Appl. Phys. 32 (1993) 2376–2379. doi:10.1143/JJAP.32.2376.

[18] M. Cole, G. Sehra, W. Gardner, J, V.K. Varadan, Development of smart tongue devices for measurement of liquid properties, IEEE Sens. J. 4 (2004) 543–550. doi:10.1109/JSEN.2004.832855.

[19] E. Gizeli, Study of the sensitivity of the acoustic waveguide sensor, Anal. Chem. 72 (2000) 5967–5972. doi:10.1021/ac000694u.

[20] M. Hoummady, A. Campitelli, W. Wlodarski, Acoustic wave sensors: design, sensing mechanisms and applications, Smart Mater. Struct. 6 (1997) 647–657. doi:10.1088/0964-1726/6/6/001.

[21] R.F. Schmitt, J.W. Allen, R. Wright, Rapid design of SAW oscillator electronics for sensor applications, Sensors Actuators B Chem. 76 (2001) 80–85. doi:10.1016/S0925-4005(01)00576-7.

[22] S. Thomas, Z. Rácz, M. Cole, J.W. Gardner, High-frequency one-port colpitts SAW oscillator for chemical sensing, in: CENICS 2013 Int. Conf. Adv. Circuits, Electron. Micro-Electronics, Barcelona, 2013: pp. 13–17.

[23] A. Castellanos, The relationship between attractive interparticle forces and bulk behaviour in dry and uncharged fine powders, 2005. doi:10.1080/17461390500402657.

[24] T.M.A. Gronewold, Surface acoustic wave sensors in the bioanalytical field: Recent trends and challenges, Anal. Chim. Acta. 603 (2007) 119–128. doi:10.1016/j.aca.2007.09.056.

[25] S. Thomas, F. Villa-Lopez, J. Theunis, J. Peters, M. Cole, J. Gardner, Particle System using Solidly Mounted Resonators, IEEE Sens. J. (2015). doi:10.1109/JSEN.2015.2512303.

[26] F. Helue, G. Rughoobur, S. Thomas, A.J. Flewitt, M. Cole, J.W. Gardner, Design and modelling of solidly-mounted resonators for low-cost particle sensing, Meas. Sci. Technol. (2015). http://dx.doi.org/.

Biographies:

Sanju Thomas received the B.Eng. degree in electronic engineering from the Visveswaraiah Technological University, Karnataka, India and MSc in Biomedical Engineering from University of Warwick, Coventry, U.K. He is currently working towards the completion of his PhD degree in acoustic biosensors and is also a research staff at the Microsensors and Bioelectronics Laboratory, Warwick University, U.K. His main research interests are Chemical Sensing and Artificial Olfaction, Acoustic wave sensors (SAW/FBAR), analog CMOS/ASIC circuit design, smart sensors and microsystems.

Marina Cole received the B.Sc. degree from the University of Montenegro, Yugoslavia, and the Ph.D. degree from Coventry University, Coventry, U.K. She joined the School of Engineering at Warwick University, Warwick, U.K., in 1996 as a Postdoctoral Research Assistant and she was appointed to a lectureship in electronic engineering in 1998. Her main research interests are integrated silicon-based sensors, SAW-based sensors, analog and mixed-signal ASICs, smart sensors, actuators, and microsystems.

Farah H. Villa-Lopez received the B.Sc. degree (Hons) in mechanical and electrical engineering from Universidad Veracruzana, Xalapa, Mexico in 2012. She is currently working towards her Ph.D. degree at the Microsensors and Bioelectronics Laboratory, University of Warwick, Coventry, UK. Her research interest includes acoustic wave sensors and microsystems.

Julian W. Gardner, BSc PhD DSc FIET SMIEEE FREng, is Professor of Electronic Engineering in the School of Engineering, Warwick University, UK. He is also the Head of Microsensors and Bioelectronics Laboratory and is author or coauthor of over 500 technical papers and patents, as well as six technical books in the area of microsensors and machine olfaction. His research interests include the modelling of silicon microsensors, chemical sensor array devices, biomimetic MEMS devices, and electronic noses. He was awarded the J. J. Thomson Medal for Outstanding Achievement in Electronics by the Institute of Engineering and Technology in 2007.

Figure Captions:

Figure 1. Basic principle of SAWR particle detection*: Schematic of a surface acoustic wave resonator based sensor with sub-micron sized particles deposited on the active sensing area.*

Figure 2. SAWR mass detection mechanism*: Cartoon of a surface acoustic wave resonator based sensor for detection of sub-micron sized particles; shown with penetration depths extending into the adjacent medium.*

Figure 3. Dual SAWR Sensor Photograph: *Optical micrograph of a 262 MHz Dual Rayleigh SAWR (free) sensor fabricated on x-propagating ST-cut quartz with aluminium electrodes for particle measurements*

Figure 4. [A] SAWR Oscillator: *Block diagram of Dual SAWR sensor, each SAWRs forming part of separate oscillator circuits.* ***[B] SAWR Transmission characteristics:*** *Attenuation vs. frequency plot of a 262 MHz free SAW resonator.*

Figure 5: Particle sensor circuitry and photograph: *[A] Schematic of SAWR oscillator including the filter, amplifier and buffer stages [B] Photograph of a dual 262 MHz (free) SAWR oscillator based sensor with surface mount amplifier, filter and buffer circuitry.*

Figure 6: Particulate Matter deposition: *[A] Experimental setup for particle deposition on SAWR sensor. [B] Photograph showing gold particles (< 1 μm diameter) deposited on the sensing area of the free SAWR particle sensor. [C] SEM image of the deposited particles.*

Figure 7. SAWR response to PM deposition: *[A] Typical frequency output of a dual free SAWR sensors in response to a deposition of ca. 0.21 ng of 0.75 μm-sized gold particles (~50 particles), on to the central active area. [B] Sensitivity analysis obtained using free SAWR devices and shorted SAWR devices for a variety of particles.*

Figure 8. SAWR Sensitivity Analysis: *Relationship between mass sensitivity and the distance from the central active region throughout the length of the free SAWR sensor along the x-axis. The dotted line indicates the axis direction starting from the central sensing region (origin) towards the outer end of the reflector.*

Figure 9. Mass-dependency of SAWR: *Linear relationship of mass-dependent differential frequency responses for a dual free SAW resonator to gold particles of diameter 0.75 μm.*

Figure 10. Effect of Particle Size on Sensitivity: *[A] Sensitivity study using particles having diameters within and outside the penetration depth of similar types of free SAWR sensor. [B] The relationship between SAWR sensitivity $\Delta f/\Delta m$ and particle diameter for one type of particle.*

Set of Figures

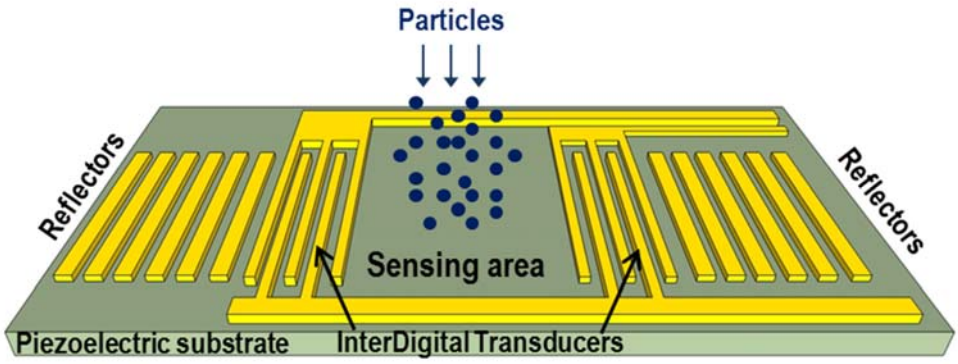

Figure 1.

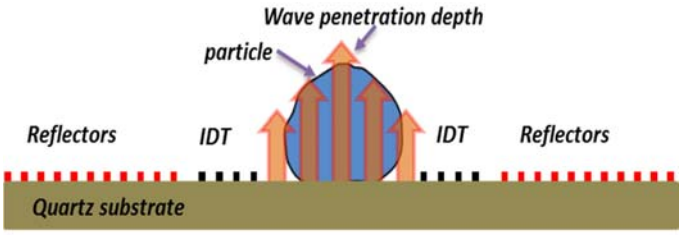

Figure 2.

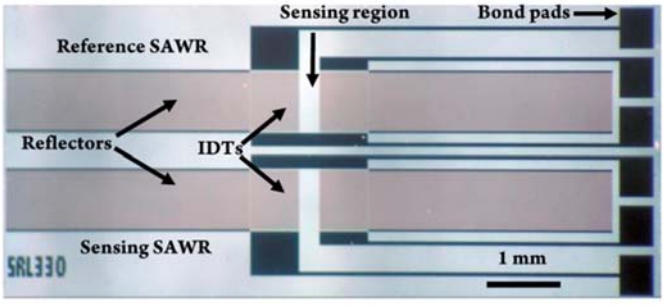

Figure 3.

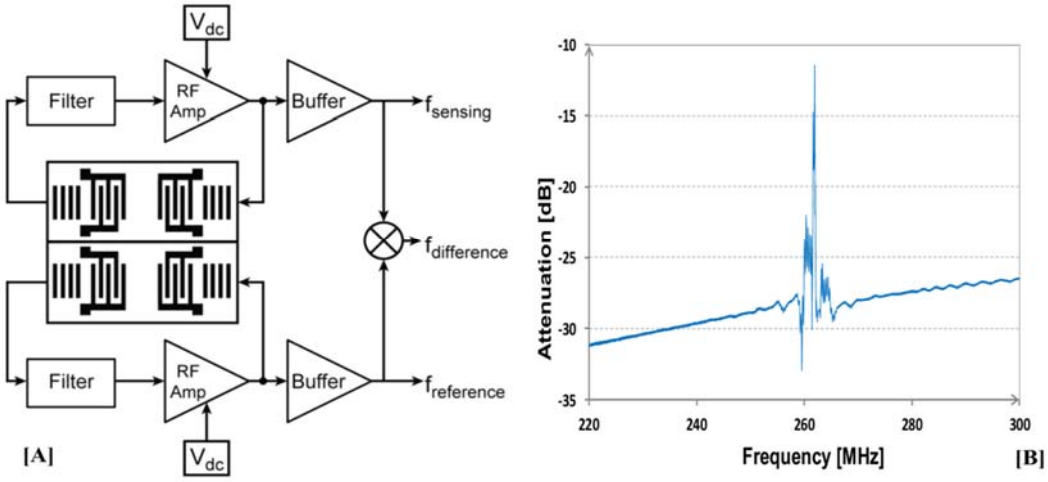

Figure 4.

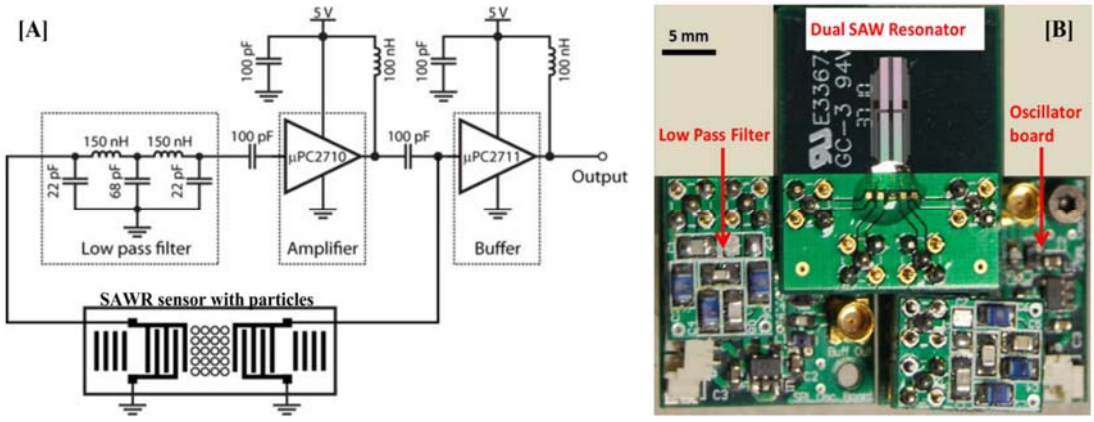

Figure 5

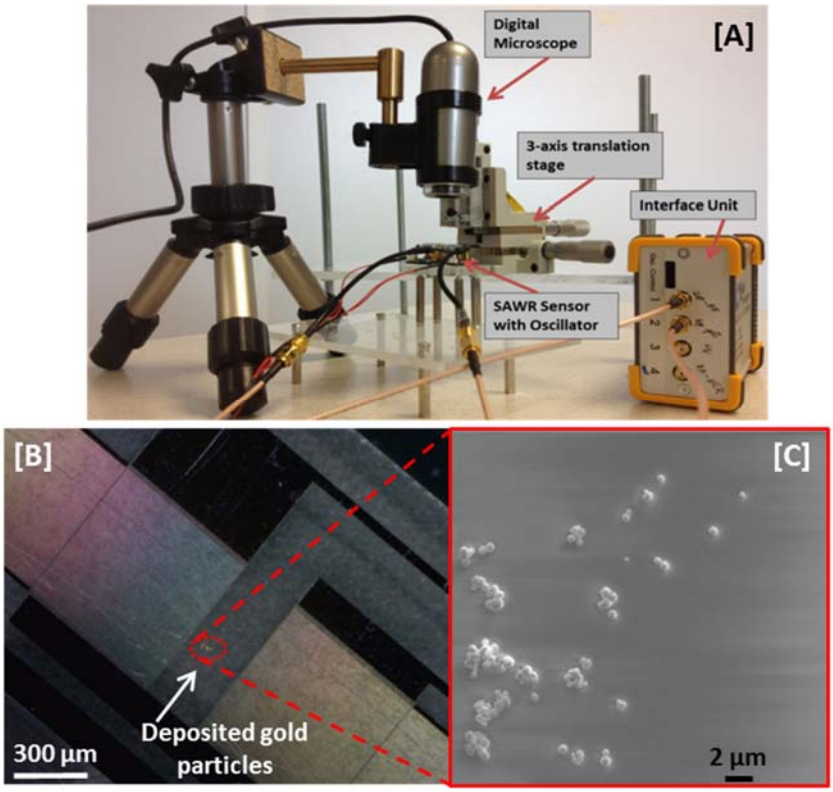

Figure 6

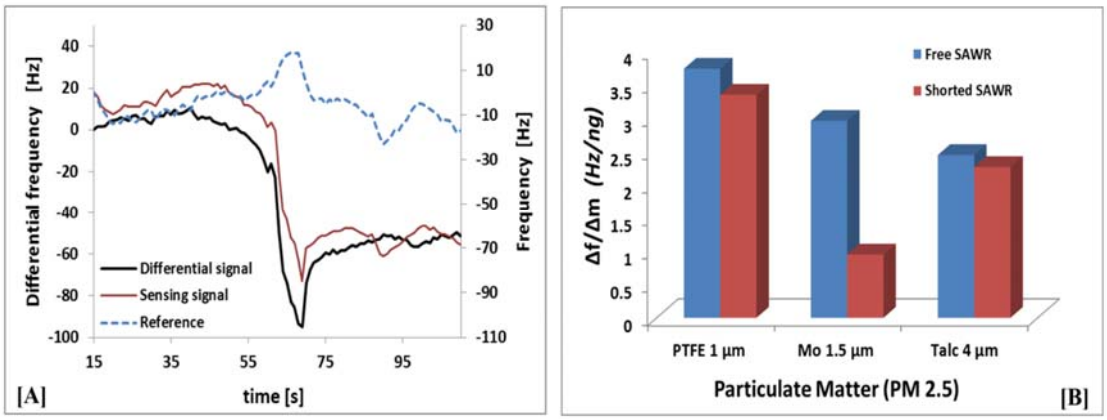

Figure 7

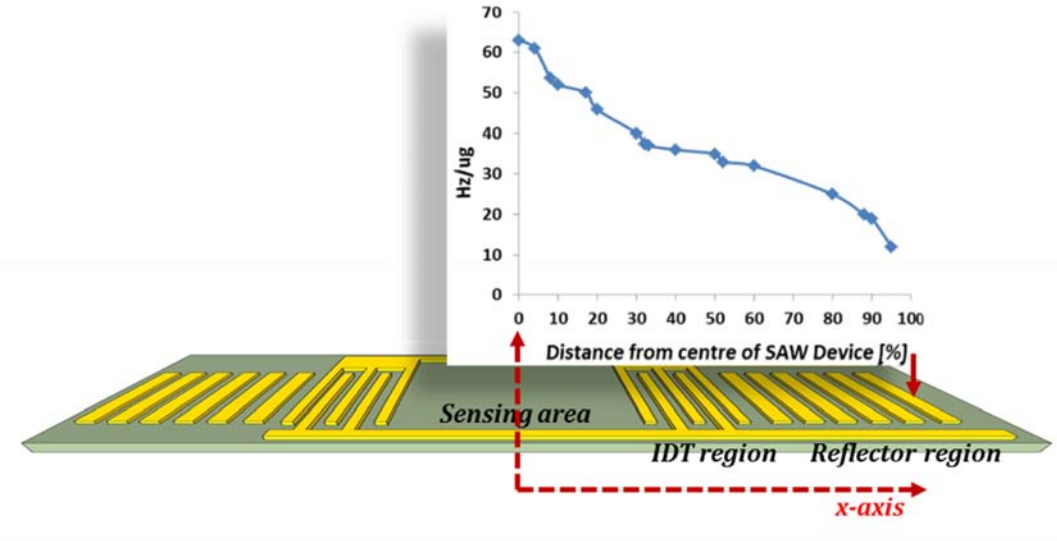

Figure 8

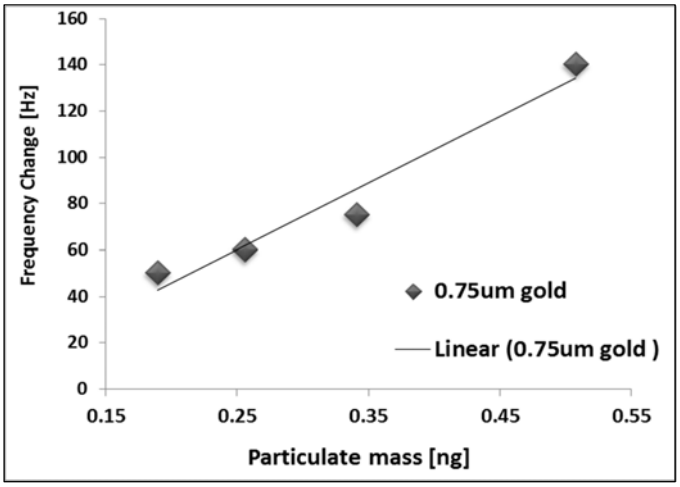

Figure 9

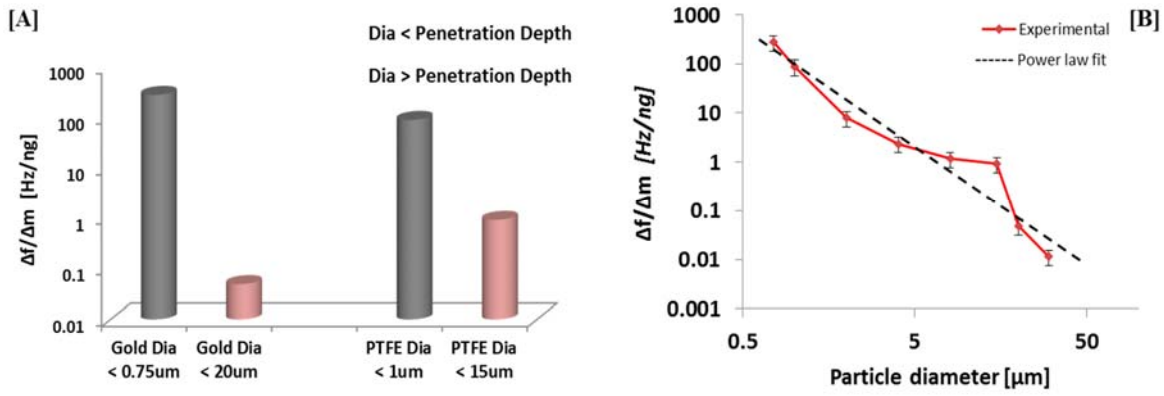

Figure 10